TÜBİTAK

Turkish Journal of Biology

http://journals.tubitak.gov.tr/biology/

Research Article

Turk J Biol
(2016) 40: 166-173
© TÜBİTAK
doi:10.3906/biy-1501-31

Biochemical characterization of wild-type and mutant (Q9F and S21Y/V22D) iron oxidases isolated from *Acidithiobacillus ferrooxidans* M1

Dilşat Nigar ÇOLAK[1], Halil İbrahim GÜLER[2], Sabriye ÇANAKÇI[1], Ali Osman BELDÜZ[1,*]
[1]Department of Biology, Faculty of Sciences, Karadeniz Technical University, Trabzon, Turkey
[2]Department of Biology, Faculty of Arts and Sciences, Artvin Çoruh University, Artvin, Turkey

Received: 12.01.2015 • **Accepted/Published Online:** 11.06.2015 • **Final Version:** 05.01.2016

Abstract: Iron oxidase, a member of the high potential iron–sulfur protein (HiPIP) family within the iron–sulfur cluster, was thought to be involved in the iron respiratory electron transport chain in *Acidithiobacillus ferrooxidans*. *A. ferrooxidans* M1 strain was isolated from Murgul copper mine. The *iro* gene of this bacterium encoding iron oxidase was cloned, and the complete nucleotide sequence was disclosed. The gene was cloned and overexpressed successfully. The highly conserved amino acid residues within the iron oxidase enzyme sequence were determined, and their Q9F and S21Y/V22D recombinants were created through site-directed mutagenesis. Wild-type and recombinant iron oxidase enzymes were purified and further characterized. The biochemical properties and kinetic parameters of wild-type and mutant enzymes were determined and compared. The optimal temperature of the wild-type enzyme was 25 °C, and maximal activity was observed at pH 4.0. The *Km* and *Vmax* values of wild-type enzyme were 0.27 ± 0.09 mM and 0.083 ± 0.01 µmol/min/mg protein, respectively. Although the mutant enzymes were almost comparable to wild-type enzyme, their maximal activities moved from pH 4.0 to pH 3.5, and pH stability of S21Y/V22D mutant was improved compared to wild type.

Key words: Acidophilic, iron oxidase, *Acidithiobacillus ferrooxidans*, site-directed mutagenesis

1. Introduction

The chemolithoautotrophic bacterium *Acidithiobacillus ferrooxidans* is of great importance in biomining operations. Among the bacteria that thrive in acidic mine drainage, it is one of the most commonly studied. *A. ferrooxidans* obtains its energy through oxidation of Fe(II) to Fe(III), with O_2 as the terminal electron acceptor (Ingledew, 1982). The oxidation mechanism of Fe(II) has been well studied, and the key components of this system have been identified. In the first step, ferrous ion is oxidized by iron oxidase, and reduced iron oxidase then transfers electrons to cytochrome c552. Cytochrome c552 transfers electrons to cytochrome c oxidase, and, finally, the electrons are transferred to molecular oxygen by the oxidase (Yamanaka and Fukumori, 1995; Zeng et al., 2010).

Iron oxidase is a member of the high redox potential iron–sulfur proteins (HiPIP), which generally function in electron transport (Fukumori et al., 1988; Cavazza et al., 1995; Iwagami et al., 1995). HiPIPs are usually isolated from purple phototrophic bacteria and form a class of small proteins (6–10 kDa) containing a $[Fe_4S_4]$ cluster. This cluster undergoes a one-electron transfer reaction between $[Fe_4S_4]^{2+}$ and $[Fe_4S_4]^{3+}$ (Cowan and Lui, 1998).

The *Iro* gene of *Acidithiobacillus ferrooxidans* has been cloned and expressed successfully in *Escherichia coli* (Kusano et al., 1992; Cavazza et al., 1995; Zeng et al., 2007), and the molecular structure of the protein has been revealed (Zeng et al., 2008). Site-directed mutagenesis results revealed that Cys20, Cys23, Cys32, and Cys45 residues are responsible for the formation of the iron–sulfur cluster (Zeng et al., 2008). Several previous reports (Rayment et al., 1992; Banci et al., 1995; Kerfeld et al., 1998; Mansy et al., 2002; Nouailler et al., 2006; Zeng et al., 2010) also proposed that the conserved aromatic residues might be responsible for the stability of the iron–sulfur cluster in HiPIP. It was also reported that Try10, Phe26, and Phe48 residues were essential to maintain the stability of the $[Fe_4S_4]$ cluster in *A. ferrooxidans* under acidic conditions (Zeng et al., 2010).

Acidithiobacillus ferrooxidans strain M1, an acidophilic bacterium newly isolated from a copper mine located in Murgul (Artvin, Turkey), has shown iron oxidase activity when grown in Fe(II). The sequence homology between HiPIP from *A. ferrooxidans* ATCC 23270 and the Iro protein from *A. ferrooxidans* M1 was 96%. In this study, the iron oxidase gene of *A. ferrooxidans* M1 was cloned

* Correspondence: belduz@ktu.edu.tr

and successfully expressed in *E. coli*. The biochemical properties and kinetic parameters of the enzyme were also determined. The two recombinants of the cloned iron oxidase, Q9F and S21Y/V22D, were created through site-directed mutagenesis and compared with wild-type iron oxidase in terms of biochemical and kinetic properties.

2. Materials and methods

2.1. Substrates and chemicals

The chemicals were purchased from Merck A.G. (Darmstadt, Germany), Sigma (St Louis, MO, USA), Fluka Chemie A.G. (Buchs, Switzerland), Acumedia Manufacturers Inc. (Baltimore, MD, USA), and Aldrich-Chemie (Steinheim, Germany). Wizard Genomic DNA Purification Kit, Wizard PlusSV Minipreps DNA Purification System, MagneHis Protein Purification System, Taq DNA Polymerase, dNTP, and all related restriction enzymes were purchased from Promega Corp. (Madison, WI, USA). All chemicals were reagent grade, and all solutions were prepared with distilled and deionized water.

2.2. Strains, vectors, and media

Acidithiobacillus ferrooxidans M1 was isolated from Murgul copper mine (Artvin, Turkey) and characterized based on its morphological, physiological, and biochemical properties and 16S rDNA sequences. *E. coli* BL21 (DE3):pLysS was purchased from Novagen (Madison, WI, USA). The plasmid vectors used were pGEMT-Easy (Promega) and pET-28a(+) (Novagen). *A. ferrooxidans* M1 was cultured aerobically at 30 °C and pH 2.5 in iron salts (TK) medium (Tuovinen and Kelly, 1973). All *E. coli* strains containing recombinant plasmids were cultured in Luria broth (LB) medium supplemented with 50 µg/mL of ampicillin or kanamycin, as appropriate, at 37 °C and pH 7.4, unless otherwise stated.

2.3. The cloning of iron oxidase gene from *A. ferrooxidans* M1

According to the manufacturer's instructions, the Wizard Genomic DNA Purification Kit (Promega Corp.) was applied for bacterial DNA extraction from *A. ferrooxidans* M1 strain. The genomic DNA was used as a template for the following PCR reactions. The iron oxidase gene was amplified by PCR using the following primers: forward primer; Iro_F: 5' - AGATATCATATGGGGACCACGCCCAAGG -3' containing a *Nde*I restriction site (CATATG) and codons for amino acids 1–5 of mature Iro protein; reverse primer; Iro_R: 5'- CAAGCTTGGAAGCAGGAGGAACTCCAGGC - 3' containing a *Hind*III restriction site (AAGCTT). PCR amplification was performed using Taq DNA polymerase, and the samples were subjected to 36 cycles of 30 s denaturation at 94 °C, 1 min annealing at 55 °C, and 1.5 min elongation at 72 °C in a Biometra Personal Cycler. The amplification products were analyzed by electrophoresis on 0.7% agarose gel and stained with ethidium bromide. The resulting PCR product was double digested with restriction enzymes, as previously defined, and ligated into a pET-28a(+) expression vector resulting in a pET/Iro plasmid. The constructed pET/Iro plasmid was transformed into *E. coli* BL21 (DE3) strain competent cells for expression purposes. The DNA sequence of the cloned iron oxidase gene was identified through sequencing, and the related gene sequence was later submitted to GenBank (GenBank accession number: KP202695).

2.4. Construction of recombinant iron oxidases

A two-step PCR was performed during the construction of recombinant iron oxidases. The plasmid pET/Iro was used as a template for the construction of mutant genes thorough PCR reaction. The following forward and antisense primers were synthesized to introduce the suggested mutations into the sequence: Q9F, 5' - GGCGGAAGTATTCTATCAGCCACACCCC - 3', the CAA encoding glutamine (Q) was replaced by TTC for phenylalanine (F); S21Y/V22D, 5' - GGATCAGTGCTATGACTGCGCCAATTTTATTGC - 3', the TCT codon for serine (S) was replaced by TAT for tyrosine (Y), and the GTC codon encoding valine (V) was replaced by GAC for aspartic acid (D). During the first-step PCR for Q9F mutation, the two separate PCR reactions were performed using Iro_F/Q9F forward and Iro_R/Q9F antisense primers, respectively. At the end of the first PCRs, a 45 bp fragment was amplified from the 5' region, and another 122 bp fragment was obtained from the 3' region of the iro gene. With the final PCR reaction, the two previously amplified fragments were combined by using the Iro_F and Iro_R primers, and the whole gene including mutant codons was obtained. The same reactions were also performed for the S21Y/V22D mutant, and the sequences of recombinant genes were verified by DNA sequencing.

Mutant genes were double digested and ligated into a pET-28a(+) expression vector resulting in pIRO(Q9F) and pIRO(S21Y/V22D). Mutant expression plasmids were later transformed into *E. coli* BL21 (DE3) for expression.

2.5. Expression and purification of recombinant iron oxidase and related recombinant proteins

Independent *E. coli* BL21 (DE3) cell lines containing pET/Iro, pIRO(Q9F), and pIRO(S21Y/V22D) plasmids were grown at 37 °C in 250 mL of LB medium supplied with 50 µg/mL kanamycin, to an OD_{600} of 0.6, respectively. The expression cells were then induced with 1 mM isopropyl-β-D thiogalactopyranoside (IPTG) and incubated for additional 4 h at 37 °C. The cells were harvested by centrifugation at 11,000 rpm for 5 min and resuspended in 50 mM Tris-HCl (pH 8.0) buffer, followed by sonication with Sartorius Labsonic M (80% amplitude, 0.6 cycles for 5

min) to release intracellular proteins. The sonicated extract was centrifuged at 14,800 rpm for 15 min to remove cell debris and obtain the cell-free extract. HisLink Protein Purification Resin (Promega) was used for purification of the proteins of interest, according to the manufacturer's instructions. The Bradford assay was used to determine the protein content with bovine serum albumin as a standard. Eluted fractions were analyzed by SDS-PAGE with 15% (v/v) acrylamide.

2.6. Determination of iron oxidase activity

Iron oxidation assays were performed by the colorimetric method modified from Harvey et al. (1955). $FeSO_4.7H_2O$ was dissolved in distilled water at a concentration of 0.025 mg/mL and used as substrate. Reaction mixture included 100 mM potassium hydrogen phthalate buffer (KHP) (pH 3.5), 5 mM ammonium peroxide sulfate, 0.025 mg/mL $FeSO_4.7H_2O$, and 25 **µ**g/mL enzyme. The final volume of the reaction was adjusted to 450 µL with distilled water. After incubation at room temperature for 5 min, 1,10-phenanthrolin (0.3%) was added to the reaction mixture, and the enzyme activity was measured spectrophotometrically at 512 nm. Likewise, the pET/Iro plasmid, an empty pET-28a(+) vector, was transformed into *E. coli* BL21 competent cells and induced over the expression period as a negative control.

2.7. Effects of temperature on enzyme activity

The effects of temperature on iron oxidase activity of both wild-type and mutant enzymes were determined spectrophotometrically using $FeSO_4.7H_2O$ as a substrate. Activity assays were performed at pH 3.5 for the temperatures 0, 4, 10, 15, 20, 25, 30, 35, 40, 45, 50, 55, 60, 65, 70, and 75 °C, and the results were revealed as relative activity (%).

2.8. Effects of pH on enzyme activity

Optimum pH levels of the enzymes were identified by using the buffer solutions from variable pH values (from pH 2.0 to pH 8.0) at 25 °C, and the relative activities of the enzymes (%) were determined spectrophotometrically at 512 nm. The following buffers were used: 100 mM potassium chloride buffer (pH 2.0), 100 mM glycine buffer (pH 3.0), 100 mM potassium hydrogen phthalate buffer (pH 3.5–4.0), 100 mM sodium acetate buffer (pH 5.0–5.5), 100 mM potassium phosphate buffer (pH 6.0–6.5–7.0), and 100 mM Tris-HCl buffer (pH 8.0).

2.9. Effects of inhibitors

The effects of various inhibitors on the oxidase activity of wild-type and mutant enzymes were assayed at 25 °C and pH 3.5 by using $FeSO_4.7H_2O$ as a substrate. Enzyme solutions were pre-incubated with DMSO 1% (v/v), β-mercaptoethanol 1% (v/v), ethanol 1% (v/v), isopropanol 1% (v/v), EDTA (5 mM), DTT (5 mM), SDS 0.1% (v/v), and Triton X-100 0.1% (v/v), consecutively. The iron oxidase activity of the enzymes without inhibitors was accepted as 100%. The residual activity (%) was measured spectrophotometrically.

2.10. Enzyme stability

The stability of the enzymes was determined by incubation in 100 mM potassium hydrogen phthalate buffer (pH 3.5) at 25 °C for 0, 5, 10, 15, 20, 25, and 30 min. The relative activities (%) of the enzymes were identified over 0.025 mg/mL $FeSO_4.7H_2O$ substrate.

2.11. Kinetic parameters

In order to quantify and reveal the enzyme characteristics of both wild-type and recombinant iron oxidases, V_{max} (µmol/min/mg), K_m (Michaelis constant, mM), and k_{cat} (1/s) values were determined from Michaelis–Menten plots of specific activities at various substrate ($FeSO_4.7H_2O$) concentrations using the OriginPro8.1 program (OriginLab data analysis and graphing software).

2.12. Statistical analysis

The variance analysis of mean values was performed with the Duncan multiple comparison test using SPSS for Microsoft Windows (v. 15.0, SPSS Inc., USA), and significance was determined at the 5% (P = 0.05) level. All analyses were repeated three times.

3. Results

3.1. Cloning of the iron oxidase gene from *Acidithiobacillus ferrooxidans* M1 and construction of the mutant plasmids

The sequence homology between iron oxidase from *A. ferrooxidans* M1 (Figure 1) and HiPIP from *A. ferrooxidans* ATCC 23270 was 96%, and HiPIP from *A. ferrooxidans* ATCC 53993 was also 96%. Iron oxidase gene from *Acidithiobacillus ferrooxidans* M1 was cloned into pET-28a(+) expression vector. In order to eliminate possible adverse effects, the signal peptide of the *iro* gene was removed during the cloning into pET-28a(+) vector. Q9F and S21Y/V22D mutants were created by site-directed mutagenesis upon the consecutive PCR reactions performed on the previously cloned iron oxidase gene. Following the DNA-sequencing–based verification of the recombinants, the expression plasmids, pIRO(Q9F) and pIRO(S21Y/V22D), were constructed by cloning the mutant genes into pET-28a(+) expression vector. In addition to the pET/Iro plasmid carrying the wild-type iron oxidase gene sequence, the mutant expression plasmids were transformed into *E. coli* BL21 (DE3) cells for expression.

3.2. Expression and purification of the wild-type and mutant iron oxidases

The expression of wild-type and mutant iron oxidases from *A. ferrooxidans* M1 in *E. coli* (BL21) was carried out at 37 °C, and 1 mM IPTG was used for the induction of gene expression in *E. coli* (BL21) cells. After a 4-h incubation at

```
  1 atgagtgagaaactgaaggaaaccggaaatgccaaggctgggaac
    M  S  E  K  L  K  E  T  G  N  A  K  A  G  N
 46 ataagccgtcgtgacatgttgaaaggtatcgccattacggccggc
    I  S  R  R  D  M  L  K  G  I  A  I  T  A  G
 91 gtcgtggctgcggggacggtggtcggagtaaatcccatcggtgcc
    V  V  A  A  G  T  V  V  G  V  N  P  I  G  A
136 gcccatgcagcgggtaattgcccggggaccacgcccaaggcggaa
    A  H  A  A  G  N  C  P  G  T  T  P  K  A  E
181 gtacaatatcagccacaccccaaggggaaggatcagtgctctgtc
    V  Q  Y  Q  P  H  P  K  G  K  D  Q  C  S  V
226 tgcgccaattttattgccccgaagtgctgtaaggtggtagccgga
    C  A  N  F  I  A  P  K  C  C  K  V  V  A  G
271 cccgtcgcacccgacgggtattgtatcgcgttcacgccgatgccc
    P  V  A  P  D  G  Y  C  I  A  F  T  P  M  P
316 gcataa 321
    A  *
```

Figure 1. The nucleotide sequence of the *iro* gene derived from *A. ferrooxidans* M1 strain (underlined letters represent substituted nucleotides).

37 °C, the cells were harvested by centrifugation at 14,800 rpm for 10 min. HisLink protein purification resin column was used for single-step purification of His-tagged iron oxidases. The purity of the enzymes was further examined by SDS-PAGE, and presence of a single band was observed, corresponding to a 5.33 kDa protein band (Figure 2). This is in agreement with the deduced molecular mass of the iron oxidase monomer.

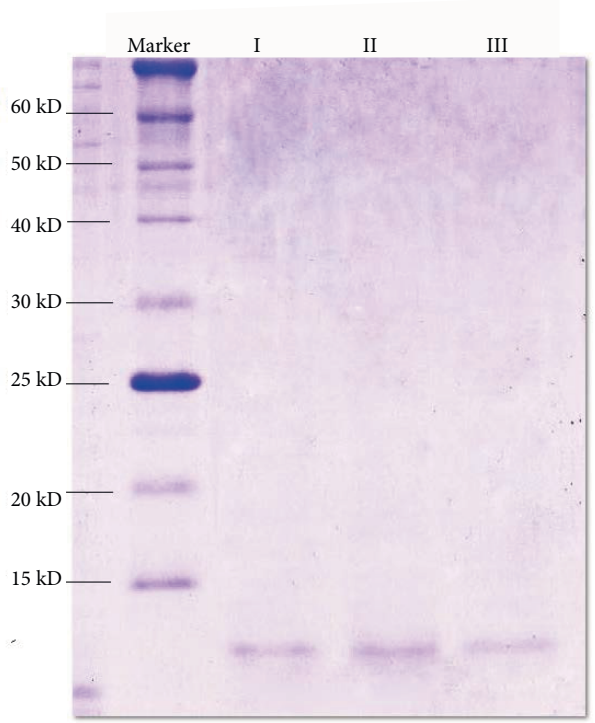

Figure 2. SDS-PAGE analyses of the His-Taq purified Iro proteins from *A. ferrooxidans* M1 wild-type, Q9F and S21Y/V22D mutants. I. Wild-type Iro, II. S21Y/V22D mutant, III: Q9F mutant.

3.3. Iron oxidase activity assays

Iron assays were performed by the colorimetric method modified from Harvey et al. (1955). A spectrophotometric determination of iron was developed earlier by Fortune and Mellon (1938) based on the formation of the iron (II)-1,10-phenanthroline complex. The iron(II)-1,10-phenanthrolin complex, which exhibits a reddish orange color, changes to a light orange color when oxidized. This complex reveals maximum absorbance at 512 nm. It was observed that Fe(II) was rapidly oxidized to Fe(III) in the presence of *A. ferrooxidans* M1 iron oxidase. The Q9F and S21Y/V22D mutants were also able to oxidize Fe(II); however, spectrophotometric analyses indicated that both Q9F and S21Y/V22D have a slightly lower oxidation effect on Fe(II) than wild-type iron oxidase (74% and 85% enzymatic activity, respectively).

3.4. Effects of temperature on iron oxidase activity

The effects of temperature on iron oxidase activity of both wild-type (*Afe*Iro-WT) and mutant (*Afe*Iro-Q9F and *Afe*Iro-S21Y/V22D) enzymes were analyzed spectrophotometrically using $FeSO_4.7H_2O$ as a substrate. *A. ferrooxidans* M1 is capable of rapid growth relative to many biomining bacteria, and this growth is generally favored within the temperature range of 25–35 °C (Rawlings, 2002). Similarly, the optimum temperature of *Afe*Iro-WT was 25 °C (Figure 3). Among wild-type and mutant proteins, *Afe*Iro-WT exhibited the highest activity, whereas the lowest activity was observed in *Afe*Iro-Q9F at 25 °C. The oxidation activity of the enzymes was conserved between 15 and 45 °C; however, a sharp drop was also observed at temperatures above 45 °C, and the activity was completely lost above 65 °C. The relative activity of *Afe*Iro-Q9F was identified as 74% and 85% in *Afe*Iro-S21Y/V22D, when compared to *Afe*Iro-WT at 25 °C. Yet the optimal

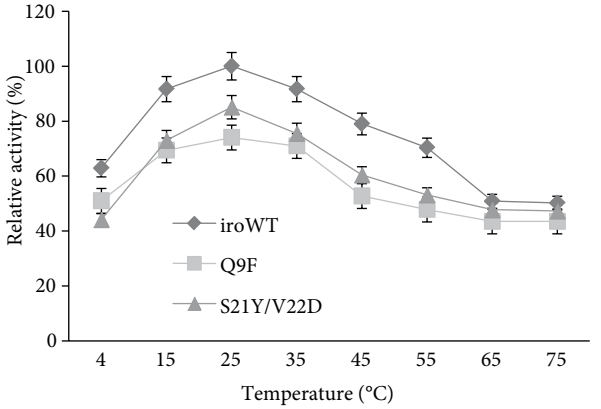

Figure 3. Optimum temperatures of iron oxidases from *Afe*Iro-WT, *Afe*Iro-Q9F, and *Afe*Iro-S21Y/V22D.

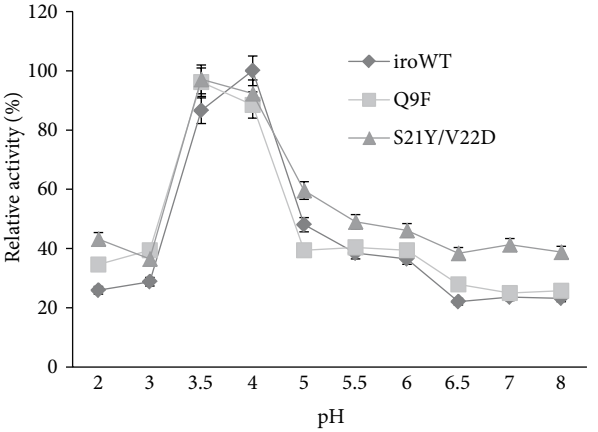

Figure 4. Optimum pH of iron oxidases from *Afe*Iro-WT, *Afe*Iro-Q9F, and *Afe*Iro-S21Y/V22D.

operating temperature of these recombinant enzymes was 25 °C, and they were also inactive above 65 °C.

3.5. Effects of pH on iron oxidase activity

The optimum growing pH of *A. ferrooxidans* M1 is 1.5–2.0. For determining the optimum pH of the iron oxidase of *A. ferrooxidans* M1, various buffers with a pH range of 2.0–8.0 were tested. The maximal activity of *Afe*Iro-WT was observed at pH 4.0 in the presence of potassium hydrogen phthalate buffer at 25 °C. A high percentage of activity was also observed at pH 3.5 with the same buffer; however, when different buffers were used for altering the pH, the enzyme lost most of its activity. At pH 5.0, the *Afe*Iro-WT enzyme lost half its enzymatic activity, and at pH 6.5 and above there was no enzyme activity identified. These results revealed that for superior oxidase activity, potassium hydrogen phthalate buffer is required. Harvey et al. (1955) and Lovenberg et al. (1963) used the same buffer for identification of iron amount by colorimetric method. Because potassium hydrogen phthalate buffer has a narrow pH range (3.5–4.0), other pH-value–related tests were performed in the presence of different buffers.

While *Afe*Iro-WT had optimum iron oxidase activity at pH 4.0, *Afe*Iro-Q9F and *Afe*Iro-S21Y/V22D mutants showed the maximal activity at pH 3.5 (Figure 4). The enzymes were capable of maintaining activity and their stability in potassium hydrogen phthalate buffer; however, activity decreased dramatically when different buffers were used. *Afe*Iro-Q9F had optimal activity at pH 3.5 and maintained 88% of its activity at pH 4.0. Like *Afe*Iro-Q9F, *Afe*Iro-S21Y/V22D recombinant enzyme also indicated optimum activity at pH 3.5 and sustained 92% of its activity at pH 4.0. The pH analyses of the enzymes revealed that *Afe*Iro-WT and *Afe*Iro-Q9F were not active at pH 6.5 and above; however, *Afe*Iro-S21Y/V22D continued operating at pH 6.5 in a range of 15%–20%, and the same range of activity was retained even at pH 8.0.

3.6 Effects of inhibitors on iron oxidase activity

The enzyme activity was markedly inhibited by β-mercaptoethanol and DTT; relative activity of the protein declined to 12% under β-mercaptoethanol and 13% by DTT. Detergents such as DMSO and Triton X-100 exhibited slight inhibition (reduced to 91% and 93%, respectively) in enzymatic activity; however, isopropanol and ethanol reduced the iron oxidase activity to 79% and 62%, respectively (Figure 5). The effects of SDS and EDTA could not be measured due to the ionic attribution of these chemicals. SDS and EDTA both interact with the substrate ($FeSO_4.7H_2O$) and inhibit the enzyme activity in this manner. The inhibition effects of all chemicals tested on *Afe*Iro-Q9F and *Afe*Iro-S21Y/V22D recombinants were similar to those identified from *Afe*Iro-WT iron oxidase.

3.7. Enzyme stability

The stability of the enzymes was tested at 25 °C with potassium hydrogen phthalate buffer (pH 3.5)

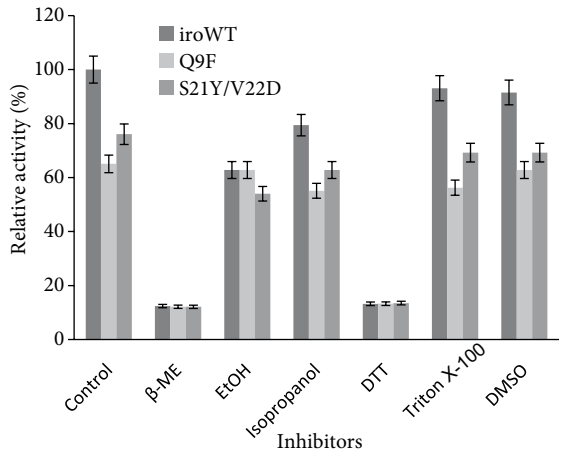

Figure 5. Effects of inhibitors on the enzyme activity.

spectrophotometrically by using a $FeSO_4.7H_2O$ substrate. All three enzymes (*Afe*Iro-WT, *Afe*Iro-Q9F, and *Afe*Iro-S21Y/V22D) revealed maximal activity in 5 min at 25 °C. However, the enzymes started to lose oxidase activity to a certain degree after 10 min (Figure 6), and the reduced activity was linear after 25 min. *Afe*Iro-WT and *Afe*Iro-Q9F maintained 80% of their specific activity after 25 min. On the other hand, *Afe*Iro-S21Y/V22D retained 88% of its specific activity after 25 min, but this difference was not remarkable based on SPSS analyses.

3.8. Kinetic parameters

Kinetic parameters were calculated using gradual concentrations of $FeSO_4.7H_2O$ (a range of 0.010–0.250 mg/mL) by taking measurements at 512 nm spectrophotometrically. *Anoxybacillus ferrooxidans* M1 wild-type iron oxidase exhibited simple Michaelis–Menten kinetics for $FeSO_4.7H_2O$ (Figure 7). The values of *K*m and *V*max were 0.27 ± 0.09 mM and 0.083 ± 0.01 µmol/min/mg, respectively. The *kcat* value was 0.29 L/s.

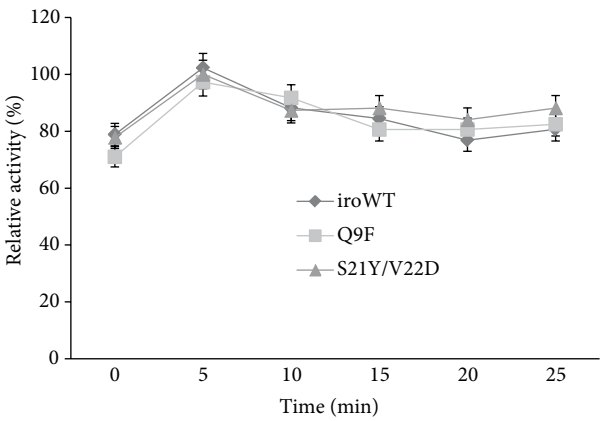

Figure 6. Enzyme stabilities of *Afe*Iro-WT, *Afe*Iro-Q9F, and *Afe*Iro-S21Y/V22D.

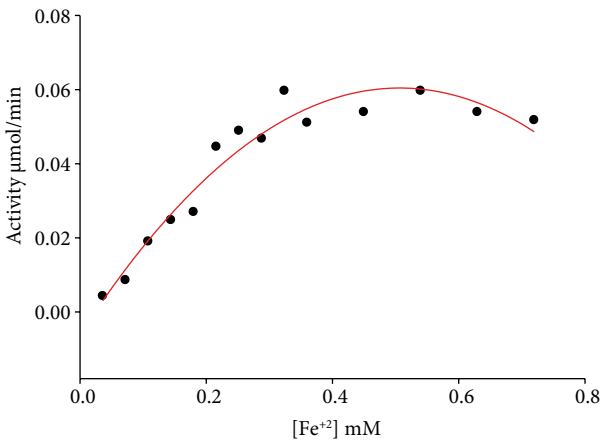

Figure 7. Michaelis–Menten plot of the *Afe*Iro-WT iron oxidase.

No significant difference was identified among the kinetic parameters of wild-type and recombinant iron oxidases. The *K*m, *V*max, and *k*cat values of *Afe*Iro-Q9F were 0.25 ± 0.07 mM, 0.087 ± 0.01 µmol/min/mg, and 0.30 L/s, respectively. The kinetic parameters of *Afe*Iro-S21Y/V22D were K_m = 0.27 ± 0.07 mM, V_{max} = 0.094 ± 0.01 µmol/min/mg, and *k*cat = 0.33 L/s. Although a small-scale increase in the catalytic efficiency (k_{cat}/Km) of the mutant enzymes (0.2 unit) was observed, the statistical analyses revealed that this increment was not significant.

4. Discussion

An iron oxidase from *Acidithiobacillus ferrooxidans* M1, isolated from Murgul copper mine, Artvin, Turkey, was cloned into pET-28a(+) expression vector, and the specific sequence of the gene was unraveled by DNA sequencing. Cloning of the *iro* gene was performed by removing its signal peptide. Almost all proteins are exported to their functional locations from cytosol, the usual site of protein synthesis. Many of these exported proteins are synthesized in a precursor form (preproteins) with an additional N-terminal amino acid extension known as a signal peptide (Beena et al., 2004). Signal peptides consist of short stretches of less than 50–60 residues (Spiess, 1995). After delivery of the protein to the correct subcellular compartment, signal peptides are normally removed by specialized membrane-associated signal peptidases (Blobel and Dobberstein, 1975). If a signal peptide is not removed after the delivery of the protein, the stability and correct folding of protein may be inhibited. When we tried to express iron oxidase with its signal peptide, there was no expression identified. For this reason, the signal peptides of the iron oxidases, consisting of 52 residues, were removed by PCR.

Kusano et al. (1992) suggested that Iro protein of *A. ferrooxidans* is composed of small polypeptide(s) with a single size around 3–6 kDa. There are also reports that the theoretical molecular mass deduced from the Iro amino acid sequence is 10.7 kDa for the precursor and 5.9 kDa for the mature protein (Bruscella et al., 2005). The molecular weight of the iron oxidase from *A. ferrooxidans* M1 was 5.33 kDa (ExPASy-Compute pl/Mw tool), which is similar to previously reported sizes. In the modelled structure of the Iro protein, the $[Fe_4S_4]$ cluster is located in the center of the protein, which is ligated by four highly conserved cysteine residues: Cys20, Cys23, Cys32, and Cys45 (Rawlings, 2001), and *A. ferrooxidans* M1 iron oxidase reveals the identical structure. Zeng et al. (2010) determined that Tyr10, Phe26, and Phe48 residues are also essential for the stability of the protein and that they are conserved in *A. ferrooxidans* M1 iron oxidase. Amino acid sequence analyses of HiPIPs from various sources revealed that Gln9, Ser21, and Val22 are highly conserved, especially

in the genus *Acidithiobacillus*. Q9F and S21Y/V22D mutations were performed by site-directed mutagenesis for determining the importance of these amino acids.

The optimum temperature of *Afe*Iro-WT was identified as 25 °C, which is similar to the optimum growing temperature of *A. ferrooxidans* (25–30 °C). Mutant proteins operate at the same optimum temperature. pH analyses of the enzymes showed that the S21Y and V22D mutations increased the pH stability of the enzyme. Statistical analyses (SPSS) also supported the related conclusions. The increment in the protein stability of S21Y/V22D mutants may be due to the aspartic acid substituted with Val22. When buried within the protein, aspartic acids are frequently involved in salt-bridges, where they pair with a positively charged amino acid to stabilize hydrogen bonds (Betts and Russell, 2003). Because positively charged residues lysine and histidine are abundant in the active site of the protein, it can be assumed that protein stability has increased thorough salt-bridges formed by aspartic acid in *Afe*Iro-S21Y/V22D.

The activity of iron oxidase was reduced by both β-ME and DTT when applied independently. β-ME reduces disulfide bonds by breaking S-S groups (Shapira and Arnon, 1969). The loss of activity through incubating the enzyme with β-ME for 10 min indicated that the protein contains disulfide linkages. It can also be concluded that S-S groups are essential for the tertiary structures of proteins. DTT is also known as an inhibitor of SH-groups and disulfide groups (S-S) (Cleland, 1964). Inhibition of iron oxidase activity by DTT supports the essentiality of S-S groups for iron oxidase protein structure and activity.

Because this is the first report about *A. ferrooxidans* iron oxidase cloned into *E. coli*, little information is available about other iron oxidases from the literature. For industrial applications, low *Km* and high *Vmax* and k_{cat} values are preferable for enzymes, and most industrial enzymes have a *Km* value between 0.01 and 100 mM. Based on current findings, we can conclude that *Afe*Iro-WT is a useful enzyme for industry. In addition, no significant difference was identified between the kinetic parameters of wild-type and mutant iron oxidases.

The fact that Fe(II) to Fe(III) oxidized proved that mutant enzymes *Afe*Iro-Q9F and *Afe*Iro-S21Y/V22D conserved the [Fe_4S_4] cluster, and the removal of the Gln9, Ser21, or Val22 residues had no effect on the stability of the iron–sulfur cluster. In the substitution of Gln9 with phenylalanine, iron oxidase lost 25% of its activity but still continued oxidizing Fe(II) to Fe(III). Glutamine is generally located in the active or binding site of the protein, and the polar side chain of Gln interacts with other polar or charged atoms (Betts and Russell, 2003). The specific activity of the *Afe*Iro-Q9F mutant slightly decreased; however, it maintained its oxidizing activity without glutamine located in the binding cleft, suggesting a lower binding capacity compared to that of wild type. *Afe*Iro-S21Y/V22D recombinant enzyme also moderately lost activity (in a range of 15%); however, the stability of the enzyme was better than that of wild-type enzyme. It was thought that the substitution of Valine 22 with aspartic acid (Asp) enhanced the stability of the enzyme due to the salt-bridges formed by aspartic acid in the protein.

In the biomining industry low pH values and high temperatures are preferable. Inducing the thermal stability of the *Acidithiobacillus ferrooxidans* M1 iron oxidase by site-directed mutagenesis will facilitate the use of the enzyme in biomining. In our experiment three amino acid residues were substituted, yet the optimum temperature of the enzyme has not changed. We decided that Gln9, Ser22, and Val22 are not essential for the activity and structure of the iron oxidase. In addition, the stability of the *Afe*Iro-S21Y/V22D was better than that of wild type for a broad range of pH values. In addition, while the activity of *Afe*Iro-S21Y/V22D was lower than wild type at pH 4.0 and 25 °C, after an incubation period of 30 min at room temperature, *Afe*Iro-S21Y/V22D was able to conserve its activity, whereas wild type did not.

This is the first study about the biochemical characteristics and kinetic parameters of an iron oxidase enzyme that was also cloned into *E. coli* BL21. The pH and thermal stability of the enzyme were enhanced by S21Y/V22D mutation. In addition, considering the difficulties experienced in the culturing conditions of *A. ferrooxidans*, successful cloning and overexpression of oxidation enzymes into rapid growing microorganisms (i.e. *E. coli*) will contribute to improving biomining-industry–based applications.

Acknowledgment

We would like to thank Karadeniz Technical University Research Foundation (grant no. 1055) for their financial support.

References

Banci L, Bertini I, Dikiy A, Kastrau DH, Luchinat C, Sompornpisut P (1995). The three-dimensional solution structure of the reduced high-potential iron–sulfur protein from *Chromatium vinosum* through NMR. Biochemistry 34: 206–219.

Beena K, Udgaonkar JB, Varadarajan R (2004). Effect of signal peptide on the stability and folding kinetics of maltose binding protein. Biochemistry 43: 3608–3619.

Betts MJ, Russell RB (2003). Amino acid properties and consequences of substitutions. In: Barnes MR, Gray IC, editors. Bioinformatics for Geneticists. Chichester, UK: Wiley, pp. 289–316.

Blobel G, Dobberstein B (1975). Transfer of proteins across membranes. I. Presence of proteolytically processed and unprocessed nascent immunoglobulin light chains on membrane-bound ribosomes of murine myeloma. J Cell Biol 67: 835–851.

Bruscella P, Cassagnaud L, Ratouchniak J, Brasseur G, Lojou E, Amils R, Bonnefoy V (2005). The HiPIP from the acidophilic *Acidithiobacillus ferrooxidans* is correctly processed and translocated in *Escherichia coli*, in spite of the periplasm pH difference between these two microorganisms. Microbiology 151: 1421–1431.

Cavazza C, Guigliarelli B, Bertrand P, Bruschi M (1995). Biochemical and EPR characterization of a high potential iron–sulfur protein in *Thiobacillus ferrooxidans*. FEMS Microbiol Lett 130: 193–200.

Cleland WW (1964). Dithiothreitol, a new protective reagent for SH groups. Biochemistry 3: 480–482.

Cowan JA, Lui SM (1998). Structure–function correlation in high-potential iron proteins. Adv Inorg Chem 45: 313–350.

Fortune WB, Mellon MG (1938). Determination of iron with o-phenanthroline. Ind Eng Chem Anal Ed 10: 60–64.

Fukumori Y, Yano T, Sato A, Yamanaka T (1988). Fe(II)-oxidizing enzyme purified from *Thiobacillus ferrooxidans*. FEMS Microbiol Lett 50: 169–172.

Harvey AE, Smart JA, Amin ES (1955). Simultaneous spectrophotometric determination of iron(II) and total iron with 1,10-phenanthroline. Anal Chem 27: 26–29.

Ingledew WJ (1982). *Thiobacillus ferrooxidans*. The bioenergetics of an acidophilic chemoautotroph. Biochim Biophys Acta 117: 683–689.

Iwagami SG, Creagh AL, Haynes CA, Borsari M, Felli IC, Piccioli M, Eltis LD (1995). The role of a conserved tyrosine residue in high-potential iron sulfur proteins. Protein Sci 4: 2562–2572.

Kerfeld CA, Salmeen AE, Yeates TO (1998). Crystal structure and possible dimerization of the high-potential iron–sulfur protein from *Chromatium purpuratum*. Biochemistry 37: 13911–13917.

Kusano T, Takeshima T, Sugawara K, Inoue C, Shiratori T, Yano T, Fukumori Y, Yamanaka T (1992). Molecular cloning of the gene encoding *Thiobacillus ferrooxidans* Fe(II) oxidase. High homology of the gene product with HiPIP. J Biol Chem 267: 11242–11247.

Lovenberg W, Buchanan BB, Rabinowitz JC (1963). Studies on the chemical nature of clostridial ferredoxin. J Biol Chem 238: 3899–3913.

Mansy SS, Xiong Y, Hemann C, Hille R, Sundaralingam M, Cowan JA (2002). Crystal structure and stability studies of C77S HiPIP: a serine ligated [4Fe-4S] cluster. Biochemistry 41: 1195–1201.

Nouailler M, Bruscella P, Lojou E, Lebrun R, Bonnefoy V, Guerlesquin F (2006). Structural analysis of the HiPIP from the acidophilic bacteria: *Acidithiobacillus ferrooxidans*. Extremophiles 10: 191–198.

Rawlings DE (2001). The molecular genetics of *Thiobacillus ferrooxidans* and other mesophilic, acidophilic, chemolithotrophic, iron or sulfur oxidizing bacteria. Hydrometallurgy 59: 187–201.

Rawlings DE (2002). Heavy metal mining using microbes. Annu Rev Microbiol 56: 65–91.

Rayment I, Wesenberg G, Meyer TE, Cusanovich MA, Holden HM (1992). Three-dimensional structure of the high-potential iron–sulfur protein isolated from the purple phototrophic bacterium *Rhodocyclus tenuis* determined and refined at 1.5 Å resolution. J Mol Biol 228: 672–686.

Shapira E, Arnon R (1969). Cleavage of one specific disulfide bond in papain. *J Biol Chem* 244: 1026–1032.

Spiess M (1995). Heads or tails—what determines the orientation of proteins in the membrane. FEBS Letters 369: 76–79.

Tuovinen OH, Kelly DP (1973). Studies on the growth of *Thiobacillus ferrooxidans*. Use of membrane filters and ferrous iron agar to determine viable numbers, and comparison with 14C02-fixation and iron oxidation as measures of growth. Arch Microbiol 88: 285–298.

Yamanaka T, Fukumori Y (1995). Molecular aspects of the electron transfer system which participates in the oxidation of ferrous ion by *Thiobacillus ferrooxidans*. FEMS Microbiol Rev 17: 401–413.

Zeng J, Geng M, Liu Y, Zhao W, Xia L, Liu J, Qiu G (2007). Expression, purification and molecular modeling of the Iro protein from *Acidithiobacillus ferrooxidans* Fe-1. Protein Expr Purif 52: 146–152.

Zeng J, Huidan J, Yuandong L, Jianshe L, Guanzhou Q (2008). Expression, purification and characterization of a high-potential iron-sulfur protein from *Acidithiobacillus ferrooxidans*. Biotechnol Lett 30: 905–910.

Zeng J, Qing L, Xiaojian Z, Hongyu M, Yiping W, Qian C, Yuandong L (2010). Functional roles of the aromatic residues in the stabilization of the [Fe_4S_4] cluster in the Iro protein from *Acidithiobacillus ferrooxidans.* J Microbiol Biotechnol 20: 294–300.